Am J Transl Res 2011;3(1):114-120
www.ajtr.org /ISSN:1943-8141/AJTR1010004

Original Article

Highly malignant intra-hepatic metastatic hepatocellular carcinoma in rats

Yang Guo[1], Rachel Klein[1], Reed A. Omary[1-3], Guang-Yu Yang[2,4], Andrew C. Larson[1-4]

[1]Department of Radiology, Northwestern University, Chicago, IL, 60611, USA; [2]Robert H. Lurie Comprehensive Cancer Center, Chicago, IL, 60611, USA; [3]Department of Biomedical Engineering, Northwestern University, Evanston, IL, 60208, USA; [4]Department of Pathology, Northwestern University, Chicago, IL, 60611, USA

Received October 25, 2010; Accepted October 29, 2010; Epub November 1, 2010; Published January 1, 2011

Abstract: Intra-hepatic metastasis is one of the major modalities that lead to the recurrence of advanced HCC. Research efforts to investigate HCC metastasis/recurrence and therapy response will require appropriate models. For our study, the main purpose was to compare two different rodent syngenic orthotopic HCC models using MRI and pathologic evidence; we specifically sought to investigate the intra-hepatic metastatic properties of HCC in Buffalo rats. *Methods*: 12 female Buffalo rats and 16 male Sprague Dawley (SD) rats were used in these studies. Subcapsular implantation of 1×10^6 McA-RH7777 and 1×10^6 N1-S1 rat hepatoma cells into the left hepatic lobe was carried out in Buffalo and SD rats, respectively. Buffalo hepatoma rats (n=5/6) and SD hepatoma rats (n=6/8) were imaged using MRI at 6-8 days after implantation. Then, another group of Buffalo HCC rats (n=6/6) and SD HCC (n=6/8) rats were scanned at 21-25 days interval post-implantation. After image acquisition, tumor sections were evaluated with H&E and CD34 staining. *Results*: Tumor induction rate for Buffalo rats was 92% (11/12) compared to 75% (12/16) for SD rats. The mean tumor size of McA-RH7777 hepatoma rats at 6-8 day interval was 1.32±0.56cm, but progressed to multiple intra-hepatic metastasis at 21-25 day interval in 6/6 rats (100%). In contrast, the mean tumor size of N1-S1 rats at early interval was 1.06±0.32cm, these progressed to only a single solid mass of 2.35±0.69cm at later interval without obvious intra-hepatic metastasis. H&E staining showed that McA-RH7777 cell induced Morris hepatoma exhibited typical trabecular growth pattern, better representative of human HCC compared to the sheet pattern of N1-S1 cell induced Novikoff hepatoma. *Conclusion*: The McA-Rh7777 rat hepatoma model was demonstrated to be a highly malignant intra-hepatic metastasis model of potential utility for HCC research.

Keywords: Hepatocellular carcinoma (HCC), rodent model, orthotopic implantation, N1-S1 rat HCC cell line, McA-RH7777 rat HCC cell line, MRI, histopathology

Introduction

Hepatocellular carcinoma (HCC) is a major health problem of worldwide significance, being the sixth most common cancer and the third leading cause of cancer-related death [1, 2]. Although curative treatments are available for early stage tumors (transplantation, resection and percutanous ablation), there is no effective therapy for those patients diagnosed at advanced stages or transitioned into advanced stages after initial therapy. Recently Sorafenib has been investigated as a new treatment option for advanced HCC [3]. Despite initial promising findings, the tumor response rate to this multi-kinase inhibitor remains low; the high frequency of HCC recurrence remains a serious problem in clinical practice.

Intra-hepatic metastasis is a critical factor leading to the recurrence of advanced HCC. This mechanism usually involves varying degrees of vascular invasion through the portal vein and/or spread to other parts of the liver. Research efforts to investigate the molecular mechanism of HCC metastasis/recurrence and new drug discoveries for advanced HCC treatments will require appropriate models. For our study, the main purpose was to compare two different rodent syngenic surgical orthotopic HCC models

using imaging evidence and pathologic evaluation at different time intervals post-implantation; we specifically sought to investigate the intra-hepatic metastatic properties of HCC in Buffalo rats. These two models have already been used in various different studies during the evaluation of anti-cancer treatments and toxicity: McA-RH7777 HCC model in Buffalo rats has been used in immunotherapy [4], liver transplantation [5] and gene therapy [6] studies; the N1-S1 rat HCC model [7] has been used in electrochemotherapy [8], biodistribution of Yttrium-90 through hepatic artery [9] studies and has been indicated as a suitable rodent HCC model for interventional studies in HCC [10, 11]. However, there have been no directed studies comparing tumor growth patterns, imaging and histology differences between these two models.

In our study, we provided MR images with corresponding hematoxylin and eosin staining and immunohistochemisty staining of CD34 to compare these two models at early and late intervals after implantation for a better understating of intra-hepatic metastatic properties in these transplanted HCC rat models. We anticipate that such information should allow future selection of a suitable model for conducting pre-clinical studies to evaluate new imaging and therapeutic approaches.

Materials and methods

Tumor cell lines and culture

The N1-S1 rat hepatoma cell line (ATCC, CRL-1603, Manassas, VA, USA) and McA-RH7777 rat hepatoma cell line (ATCC, CRL-1601, Manassas, VA, USA) were obtained and cultured in Dulbecco's Modified Eagle's Medium (DMEM, ATCC, Manassas, VA, USA) supplemented with 10% fetal bovine serum (Sigma-Aldrich, MO, USA) and 0.1% gentamycin (Sigma-Aldrich, MO, USA). N1-S1 cells were maintained in suspension while McA-RH7777 cells were loosely adherent in 75cm^2 culture flasks at 37°C in a humidified atmosphere containing 5% CO_2. The viability of the cells was tested with Trypan blue staining (confirming > 90% cell viability for each tumor implantation procedure).

Animals

All studies were approved by our institutional animal care and use committee and were performed in accordance with institutional guidelines. Twelve female Buffalo rats aging initially from 55 days to 60 days (Charles River Laboratories, Wilmington, MA, USA) and sixteen male Sprague Dawley (SD) rats (Charles River Laboratories, Wilmington, MA, USA) weighting initially 301-325g were used for these studies.

Tumor inoculation

Buffalo rats were anesthetized with isoflurane at an induction dose of isoflurane/oxygen medical mixture (5% isoflurane, oxygen medical 3 L/min) and maintained at a dose of isoflurane/oxygen mixture (1–2% isoflurane, oxygen 3 L/min). SD rats were anesthetized with a hind limb injection of Ketamine (75-100 mg/kg) and Xylazine (2-6 mg/kg). After anesthesia, a mini-laporatomy was performed on each rat and the left hepatic lobe was exposed on a sterile compress. 1x10^6 McA-RH7777 rat hepatoma cells were visually injected under the hepatic capsule into this lobe in Buffalo rats; 1x10^6 N1-S1 hepatoma cells were injected using the same protocol in SD rats (**Figure 1**). A pale whitish coloring could be seen at the point of injection under the hepatic capsular. A gentle compression was applied for 15 seconds with a cotton applicator to avoid bleeding and reflux of the cells. Then

Figure 1. Subcapsular implantation of 1×10^6 N1-S1 rat HCC cells into the left hepatic lobe of Sprague Dawley rats.

the abdominal incisions were closed with 2-layer technique followed by topical application of antibiotic ointment and Metacam injection (1-2mg/kg, SQ). Animals were returned to storage facilities for the duration of the follow-up intervals after implantation.

MRI protocols

All MRI studies were performed using a 3.0T Magnetom Trio clinical scanner (Siemens Medical Solutions, Erlangen, Germany) with custom-built rodent receiver coil (Chenguang Med. Tech. Co., Shanghai, China). Along both coronal and transverse orientations, T2-weighted (T2W), T1-weighted (T1W), and proton-density weighted (PD-W) spin echo (TSE) imaging was performed with a multi-slice acquisition providing complete coverage of the entire liver. All scans were performed using a 150mm FOV, 2.0mm slice-thickness, 3 signal averages, 256 matrix (0.6x0.6 mm^2 in-plane voxel size), repetition and echo time (TR/TE) = 3500/60ms for T2W imaging, TR/TE = 300/8ms for T1W imaging, and TR/TE = 3500/8ms for PD-W imaging. The MRI measurements were performed at 6-8 days and 21-25 days intervals after implantation.

Image Analysis

All measurements were performed offline using the ImageJ software package (http://rsb.info.nih.gov/ij/). All coronal and axial orientation DICOM format images for each animal were reviewed according to RECIST criteria [12] with the maximum tumor diameter measured within T2W TSE images. For N1-S1 rat hepatoma, the tumor maximum diameter at 6-8 days interval and 21-25 days interval were measured and compared. For McA-RH7777 rat hepatoma, the total tumor nodules were visualized by MRI and confirmed at gross anatomy.

Histology

After MRI studies, each rat was euthanized with intravenous injection of Euthasol at a dose of 150 mg/kg and bilateral thoracotomy. 2-3 sections across the tumors were sampled and fixed in 10% formaldehyde solution; these tissue sections were then embedded in paraffin for H&E staining and CD34 immunohistochemistry staining.

Tumor morphology and cytology properties were evaluated on H&E slides, including tumor growth pattern, capillarization (microvessel structure), cellular atypia, mitotic activity and intra-tumor necrosis [13, 14]. The mitotic activity, an indicator of tumor aggressiveness, was counted as the number of mitoses in 10 high power fields (400×) [15]. CD34 staining was performed as a malignant tumor neovascularization marker highlighting the regions of sinusoidal capillarization [16]. CD34 slides were digitized with ×100 optical magnification using a multi-channel automated imaging system (TissueGnostics, Vienna, Austria). Quantitative analysis of tumor angiogenesis was performed within each tumor region using Matlab software (The Math Works Inc., Natick, MA) that differentiated CD34 stained areas from hepatoma areas based on color differentiation. Tumor neovascular maps were generated based on color differentiated images. Tumor micro-vessel density (MVD) was expressed as the ratio of CD34 positive stained area per total tumor area.

Statistics

All statistics were performed using the SPSS statistical software package (SPSS, Chicago, IL, USA). The tumor cell mitosis activities were compared with a two independent samples t-test to examine differences between McA-RH7777 hepatoma rats and N1-S1 hepatoma rats between the 6-8 days and 21-25 days intervals after implantation, respectively. Tests were considered statistically significant with a p-value < 0.05.

Results

The tumor induction rate for Buffalo rats was 92% (11/12) compared to 75% (12/16) for SD rats. No severe post-procedure complications were observed in either rat model (bleeding, marked inactivity, internal infection, etc). No mortalities were observed during the follow-up interval.

MR imaging

Both McA-RH7777 rat hepatoma and N1-S1 rat hepatoma were hyper-intense within T2-wieghted images, hypo-intense within T1-wieghted images and typically iso-intense within proton-density weighted images.

McA-RH7777 HCC cells transplanted into Buf-

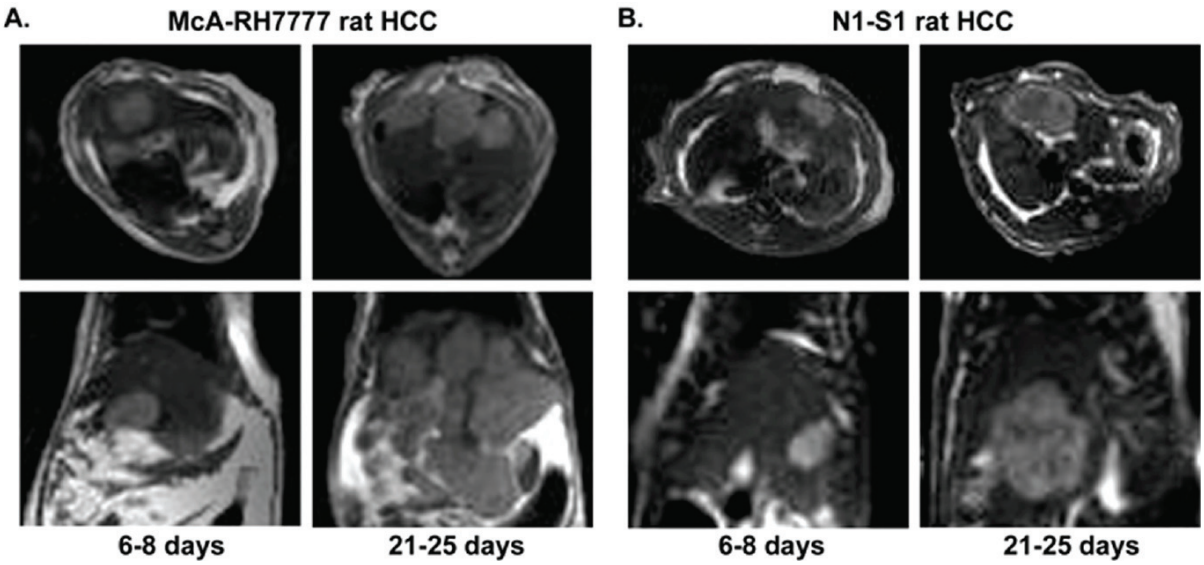

Figure 2. Transverse and coronal T2-weighted MR images at 6-8 day and 21-25 day intervals in McA-RH7777 rat HCC (**A**) and N1-S1 rat HCC (**B**) models.

falo rats (n=5/6) grew from one single nodule of 1.32±0.56cm at 6-8 days interval and progressed to multiple intra-hepatic metastasis which counted up to 5-10 nodules (n=6/6) at 21-25 days interval post-implantation. In contrast, each SD rat (n=6/8) developed only a single N1-S1 hepatoma with sizes 1.06 ± 0.32cm at 6-8 days interval; these progressed in size to 2.35 ± 0.69cm without any observable intra-hepatic metastasis (n=6/8) at 21-25 days interval post-implantation. Transversal and coronal T2W TSE images at 6-8 days and 21-25 days intervals for Buffalo rats and SD rats are shown in **Figure 2A** and **Figure 2B**, respectively.

H&E staining

H&E slides showed that each McA-RH7777 hepatoma were a solid mass with an invasive border. Morphologically, these tumors exhibited a typical trabecular growth pattern (**Figure 3A**). Cytologically, tumor cells were epithelial in shape with moderate cytological atypia with mitotic activity of 169.6±14.0 mitosis/10HPF within the 89±5% percent viable tumor at the 6-8 days interval. Focal tumor necrosis was observed with 11±5% central necrosis due to tumor ischemia when tumor maximum diameter was larger than 1.0cm. At the 21-25 days interval, tumor mitotic activity increased to 236.3±10.3mitosis/10HPF within the 75±11% percentage viable tumor. Focal intra-tumor necrosis increased to 25% percent inside the tumor due to rapid progression.

Gross anatomy for N1-S1 transplanted hepatoma showed only one single nodule progressing locally without observable intra-hepatic or peritoneal wall metastasis. H&E staining slides showed that N1-S1 Novekoff hepatoma grew in a solid sheet pattern compared to McA-RH7777 Morris hepatoma's trabecular pattern (**Figure 3B**). At 6-8 days interval, a 90±4% viable tumor was observed with mitotic activity of 73.0±18.9mitosis/10HPF and at 21-25 days interval, 68±8% viable tumor with 32±8% focal necrosis due to tumor ischemia; at this delayed interval we observed a mitotic activity of 113.1±35.6mitosis/10HPF. The difference in mitotic activity between McA-RH7777 hepatoma and N1-S1 hepatoma was statistically significant at each interval ($p<0.0001$).

CD34 staining

Diffuse positive staining for CD34 in sinusoidal-like vessels indicated the process of tumor angiogenesis in both McA-RH7777 hepatoma and N1-S1 hepatoma models. Representative CD34 staining image are shown in **Figure 3** demonstrating CD34 expression (brown staining) in the tumor region (blue staining). Digitalized CD34

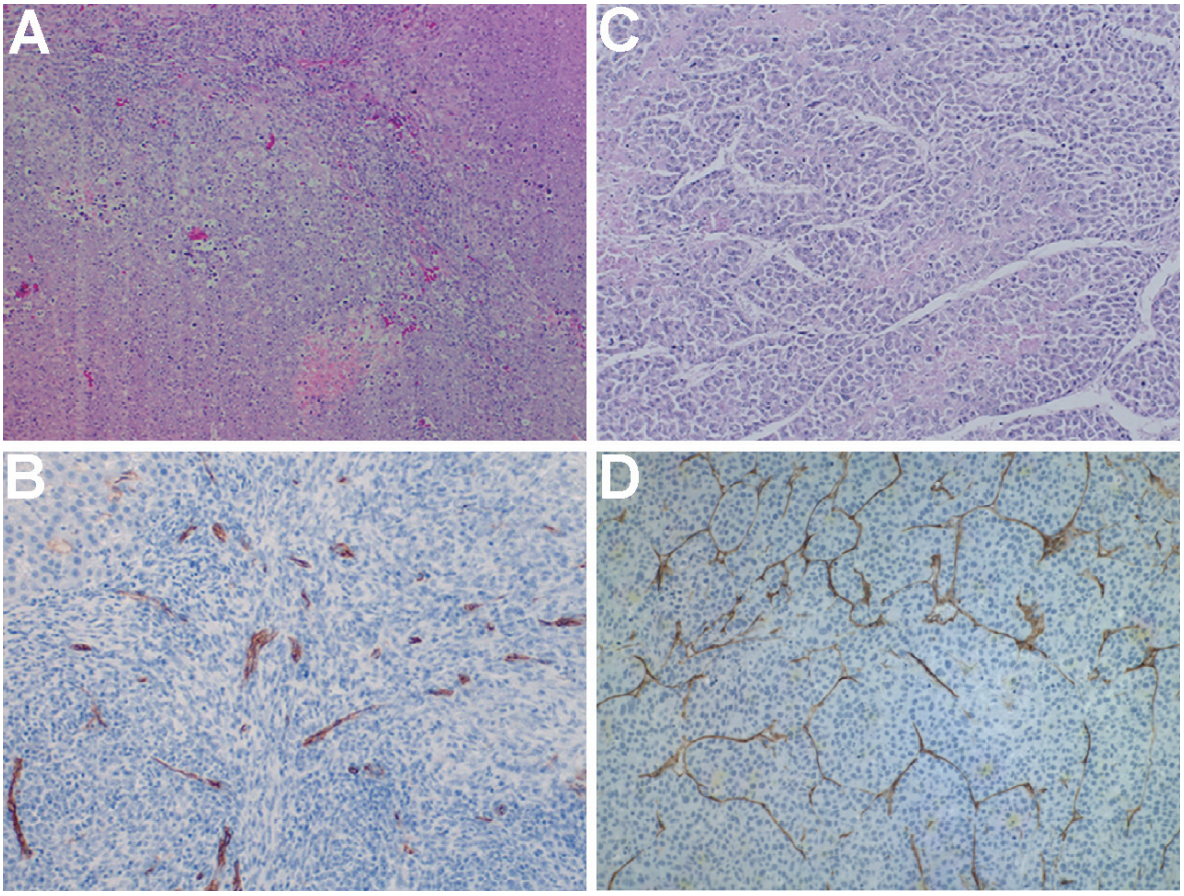

Figure 3. HE staining (**A, C**) and CD34 staining (**B, D**) images from N1-S1 rat hepatoma (**A, B**) and McA-RH7777 rat hepatoma (**C, D**).

images were transformed into binary black (CD34 positive) and white images based on color differentiation (brown and blue). Representative reconstructed tumor neovasular maps for rat N1-S1 hepatoma and McA-RH7777 hepatoma at an early interval (1.0cm diameter tumor) are shown in **Figure 4**, clearly demonstrating that the McA-RH7777 hepatoma model is more hyper-vascular compared to the N1-S1 hepatoma.

Discussion

Using MRI and histological measurements we compared two rodent HCC models and demonstrated that McA-RH7777 Morris hepatoma can serve as a highly malignant intra-hepatic metastasis model of HCC. We observed that Morris hepatoma in the Buffalo rats demonstrated significantly greater levels of neovascularization, metastasis, mitotic activity than Novikoff hepatoma in SD rats; Morris hepatoma also exhibited growth patterns more closely representative of those observed in human HCC.

These two rat HCC models used the same methodology: 1) the origin of the implanted tumor (rat hepatoma cell lines), the type of the sample (suspension of malignant cells maintained in culture) and the anatomical site of implantation (the left hepatic lobe). However, a significant difference between these two rodent models was found; all the Buffalo rats developed intra-hepatic metastasis at 21-25 days interval (n=6/6) while there was no intra-hepatic metastasis were observed in SD rats (n=6/6). Although both McA-RH7777 and N1-S1 hepatoma rats developed a single nodule at an early interval after implantation, the Morris7777 hepatoma in Buffalo rats would develop multiple intra-hepatic metastases at a later interval (21-25 days) after implantation. Also, morphologically,

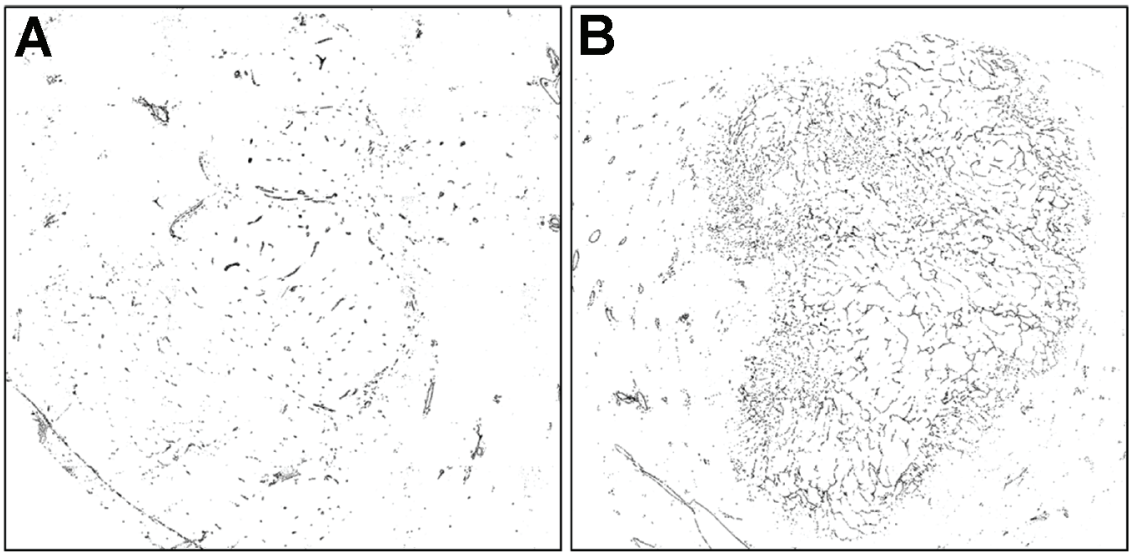

Figure 4. Representative N1-S1 rat HCC (**A**) and McA-RH7777 rat HCC (**B**) tumor neovasular map based on color differentiation from CD34 staining (black, CD34 expression).

McA-RH7777 hepatoma grew in a trabecular pattern which preserved more histological appearance of human HCCs compared to the sheet pattern of N1-S1 hepatoma. Human HCCs exhibit either microtrabecular growth pattern when occurring in normal liver tissue or macrotrabecular pattern when occurring in cirrhotic livers [17]. The mitotic activity of McA-RH7777 rat hepatoma was significantly higher than N1-S1 rat hepatoma, which indicated the McA-RH7777 model was more aggressive histologically. In sum, these findings suggested that the McA-RH7777 rat HCC model may be suitable to serve as a highly malignant intra-hepatic metastasis hepatoma model in pre-clinical studies.

There were two minor technical differences found in these two models: 1) anesthesia: SD rats were well anesthetized under Ketamine and Xylazine, but Buffalo rats were quite sensitive to Xylazine leading to respiratory arrest but would be well anesthetized under isoflurane inhalation. 2)the amount of cell suspension medium: initially we used 0.05ml complete medium to suspend the $1x10^6$ N1-S1 HCC cells which contributed to 50% (2/4) tumor induction compared to 100% (4/4) tumor induction rate when suspended in 0.20 ml complete medium. Similar results were observed in another 4 SD rats, which might suggest a larger amount of suspension medium (0.20ml) may be necessary for improved tumor inoculation.

HCC frequently manifests as multiple lesions in the liver. The multiplicity of the lesions has been explained by a multi-centric origin of HCC or intra-hepatic metastasis [18, 19]. Most recurrence of HCC in non-cirrhotic liver is considered to be due to intra-hepatic metastasis or to be de novo hepatocarcinogenesis. Also, intra-hepatic metastasis is more often observed in distinct and poorly differentiated nodular tumor types. The syngenic orthotopic implantation method used in these two rodent hepatoma models preserved the influence of the immune system and other tumor-host interactions compared to the xenograft models in immuno-compromised rodents [20]. Moreover, tumor inoculation by intra-hepatic injection of the tumor cells mimics the progression of human HCC which causes progressive infiltration of the liver. However, the clinical relevance of these transplanted rat hepatoma models still depends on their molecular features and how well these mimic human-like HCC characteristics. The latter aspect was not investigated in the current study and remains a limitation that should be examined in the future.

Acknowledgement

This publication was made possible by Grant

Number CA134719 from the National Institutes of Health (NIH). Its contents are solely the responsibility of the authors and do not necessarily represent the official view of the NIH.

Please address correspondence to: Andrew C. Larson, PhD, Departments of Radiology and Biomedical Engineering, Northwestern University Feinberg School of Medicine, 737 N. Michigan Ave, 16th Floor, Chicago, IL 60611, USA. Telephone: + 01-1-3129263499, Fax: +01-1-3129265991, E-mail: a-larson@northwestern.edu

References

[1] Parkin DM, Bray F, Ferlay J and Pisani P. Global cancer statistics, 2002. CA Cancer J Clin 2005; 55: 74-108.

[2] Thomas MB and Zhu AX. Hepatocellular carcinoma: the need for progress. J Clin Oncol 2005; 23: 2892-2899.

[3] Abou-Alfa GK, Schwartz L, Ricci S, Amadori D, Santoro A, Figer A, De Greve J, Douillard JY, Lathia C, Schwartz B, Taylor I, Moscovici M and Saltz LB. Phase II study of sorafenib in patients with advanced hepatocellular carcinoma. J Clin Oncol 2006; 24: 4293-4300.

[4] Maggard M, Meng L, Ke B, Allen R, Devgan L and Imagawa DK. Antisense TGF-beta2 immunotherapy for hepatocellular carcinoma: treatment in a rat tumor model. Ann Surg Oncol 2001; 8: 32-37.

[5] Ogawa T, Tashiro H, Miyata Y, Ushitora Y, Fudaba Y, Kobayashi T, Arihiro K, Okajima M and Asahara T. Rho-associated kinase inhibitor reduces tumor recurrence after liver transplantation in a rat hepatoma model. Am J Transplant 2007; 7: 347-355.

[6] Schmitz V, Barajas M, Wang L, Peng D, Duarte M, Prieto J and Qian C. Adenovirus-mediated CD40 ligand gene therapy in a rat model of orthotopic hepatocellular carcinoma. Hepatology 2001; 34: 72-81.

[7] Novikoff AB. A transplantable rat liver tumor induced by 4-dimethylaminoazobenzene. Cancer Res 1957; 17: 1010-1027.

[8] Jaroszeski MJ, Coppola D, Pottinger C, Benson K, Gilbert RA and Heller R. Treatment of hepatocellular carcinoma in a rat model using electrochemotherapy. Eur J Cancer 2001; 37: 422-430.

[9] Wang SJ, Lin WY, Lui WY, Chen MN, Tsai ZT and Ting G. Hepatic artery injection of Yttrium-90-lipiodol: biodistribution in rats with hepatoma. J Nucl Med 1996; 37: 332-335.

[10] Garin E, Denizot B, Roux J, Noiret N, Lepareur N, Moreau M, Mesba H, Laurent JF, Herry JY, Bourguet P, Benoit JP and Lejeune JJ. Description and technical pitfalls of a hepatoma model and of intra-arterial injection of radiolabelled lipiodol in the rat. Lab Anim 2005; 39: 314-320.

[11] Ju S, McLennan G, Bennett SL, Liang Y, Bonnac L, Pankiewicz KW and Jayaram HN. Technical aspects of imaging and transfemoral arterial treatment of N1-S1 tumors in rats: an appropriate model to test the biology and therapeutic response to transarterial treatments of liver cancers. J Vasc Interv Radiol 2009; 20: 410-414.

[12] Therasse P, Arbuck SG, Eisenhauer EA, Wanders J, Kaplan RS, Rubinstein L, Verweij J, Van Glabbeke M, van Oosterom AT, Christian MC and Gwyther SG. New guidelines to evaluate the response to treatment in solid tumors. European Organization for Research and Treatment of Cancer, National Cancer Institute of the United States, National Cancer Institute of Canada. J Natl Cancer Inst 2000; 92: 205-216.

[13] Quaglia A, Jutand MA, Dhillon A, Godfrey A, Togni R, Bioulac-Sage P, Balabaud C, Winnock M and Dhillon AP. Classification tool for the systematic histological assessment of hepatocellular carcinoma, macroregenerative nodules, and dysplastic nodules in cirrhotic liver. World J Gastroenterol 2005; 11: 6262-6268.

[14] Lauwers GY, Terris B, Balis UJ, Batts KP, Regimbeau JM, Chang Y, Graeme-Cook F, Yamabe H, Ikai I, Cleary KR, Fujita S, Flejou JF, Zukerberg LR, Nagorney DM, Belghiti J, Yamaoka Y and Vauthey JN. Prognostic histologic indicators of curatively resected hepatocellular carcinomas: a multi-institutional analysis of 425 patients with definition of a histologic prognostic index. Am J Surg Pathol 2002; 26: 25-34.

[15] Terminology of nodular hepatocellular lesions. International Working Party. Hepatology 1995; 22: 983-993.

[16] Fox SB and Harris AL. Histological quantitation of tumour angiogenesis. Apmis 2004; 112: 413-430.

[17] Kishi K, Shikata T, Hirohashi S, Hasegawa H, Yamazaki S and Makuuchi M. Hepatocellular carcinoma. A clinical and pathologic analysis of 57 hepatectomy cases. Cancer 1983; 51: 542-548.

[18] Matsumoto Y, Fujii H, Matsuda M and Kono H. Multicentric occurrence of hepatocellular carcinoma: diagnosis and clinical significance. J Hepatobiliary Pancreat Surg 2001; 8: 435-440.

[19] Akihiro Toyosaka EO, Masao Mitsunobu, Takeshi Oriyama, Norio Nakao, Koui Miura. Intrahepatic Metastases in Hepatocellular Carcinoma: Evidence for Spread Via the Portal Vein as an Efferent Vessel. American Journal of Gastroenterology 1996; 91: 1610-1615.

[20] Kramer MG. Evaluation of hepatocellular carcinoma models for preclinical studies. Drug Discovery Today: Disease Models (Cancer) 2005; 2: 41-49.